Journal of Biological Physics **28:** 163–172, 2002.

Infrared Study of Carbon Monoxide Migration among Internal Cavities of Myoglobin Mutant L29W

G.U. NIENHAUS[1,2] and K. NIENHAUS[1]
[1]*Department of Biophysics, University of Ulm, D-89069 Ulm, Germany*
[2]*Department of Physics, University of Illinois at Urbana-Champaign, 1110 West Green Street, Urbana, IL 61801 3080, USA, Email: uli@uiuc.edu.*

Abstract. Myoglobin, a small globular heme protein that binds gaseous ligands such as O_2, CO and NO reversibly at the heme iron, provides an excellent model system for studying structural and dynamic aspects of protein reactions. Flash photolysis experiments, performed over wide ranges in time and temperature, reveal a complex ligand binding reaction with multiple kinetic intermediates, resulting from protein relaxation and movements of the ligand within the protein. Our recent studies of carbonmonoxy-myoglobin (MbCO) mutant L29W, using time-resolved infrared spectroscopy in combination with x-ray crystallography, have correlated kinetic intermediates with photoproduct structures that are characterized by the CO residing in different internal protein cavities, so-called xenon holes. Here we have used Fourier transform infrared temperature derivative spectroscopy (FTIR-TDS) to further examine the role of internal cavities in the dynamics. Different cavities can be accessed by the CO ligands at different temperatures, and characteristic infrared absorption spectra have been obtained for the different locations of the CO ligand within the protein, enabling us to monitor ligand migration through the protein as well as conformational changes of the protein.

Key words: FTIR spectroscopy, ligand binding, myoglobin, temperature derivative spectroscopy

1. Introduction

Proteins are complex macromolecules that perform an impressive variety of functional tasks in living systems. Within their native folds, they can assume a large number of different conformations that are frequently represented by local minima in a rugged energy landscape. For a quantitative, predictive understanding of protein function, elucidation of the energy landscape, with its functionally important intermediate states and the barriers separating them, is a prerequisite. Detailed investigations of this kind are only feasible for a few well selected model systems. Among these, myoglobin (Mb), a small monomeric heme protein of about 18 kD, has been particularly popular. Its polypeptide chain consists of 153 amino acids, folded into eight α-helices. They are connected by loops and wrapped around a heme prosthetic group, which is covalently linked to the proximal histidine (H93) through its central Fe^{2+} ion [1–3]. Small ligands such as O_2, NO or CO bind revers-

ibly to the heme iron from an internal cavity, the distal heme pocket. Experimental studies as well as computer simulations have revealed an enormous complexity in this comparatively simple biological process [4, 5].

Flash photolysis experiments on carbonmonoxymyoglobin (MbCO) and oxymyoglobin (MbO_2) over wide time and temperature ranges have shown that ligand binding involves multiple intermediate states [4]. In recent years, evidence has mounted that these correspond to transient binding sites of ligands in internal protein cavities [6], the so-called 'xenon' holes [7]. The clearest insights have been provided by x-ray structure analyses of photolyzed MbCO at cryogenic temperatures with selective trapping of photoproduct intermediates [8–13]. From these studies, a picture has emerged for physiological ligand binding in which the ligand, after entering the protein from the solvent, shuttles among the various cavities many times before either binding to the heme iron or exiting again into the solvent.

Figure 1 shows essential features of the L29W MbCO crystal structure at 105 K, including the heme group and the sidechains of H64 and W29 as well as the CO ligand in the bound and the various photoproduct states [10, 12]. The bound ligand is labelled A_1. The sidechains of the distal histidine (H64) and tryptophan B10 (W29) in MbCO are depicted in dark grey. Also shown are the CO locations in the photoproduct states B on top of heme pyrrol C and C' in the so-called Xe4 cavity. Both these photoproduct states can be populated upon photolysis below $\sim$180 K. Apart from the movement of the central iron by 0.3 Å out of the mean heme plane, no other significant structural changes occur. After photodissociation above $\sim$180 K, the ligand occupies state D on the proximal side (Xe1 cavity), and the sidechains of H64 and W29 rearrange markedly (shown in light grey) so that the W29 indole ring adopts the same conformation as in the room temperature bound-state structure [14].

Knowledge of these intermediate states is a prerequisite for understanding the dynamic aspects of the binding reaction, i.e. the temporal sequence of ligand transitions among the various sites as well as the accompanying protein fluctuations and relaxations. While it is, in principle, possible to observe protein motions and CO transitions among the different cavities by time-resolved x-ray crystallography [15], such experiments are, in practice, very difficult and limited in their dynamic range. Spectroscopic experiments are often easier to perform, provided that a suitable marker exists to study the dynamics. Here we show that the infrared absorption of the photodissociated CO is sensitively dependent on its local environment and can be used to track CO migration among the different protein cavities.

2. Methods and Materials

Sperm whale myoglobin mutant L29W was expressed in *E. coli* and purified as described previously [16]. For the experiments, lyophilized protein powder was dissolved at a concentration of $\sim$15 mM in cryosolvent (75% glycerol/25% potassium phosphate buffer (v/v), pH 7.5), stirred under a CO atmosphere and reduced with

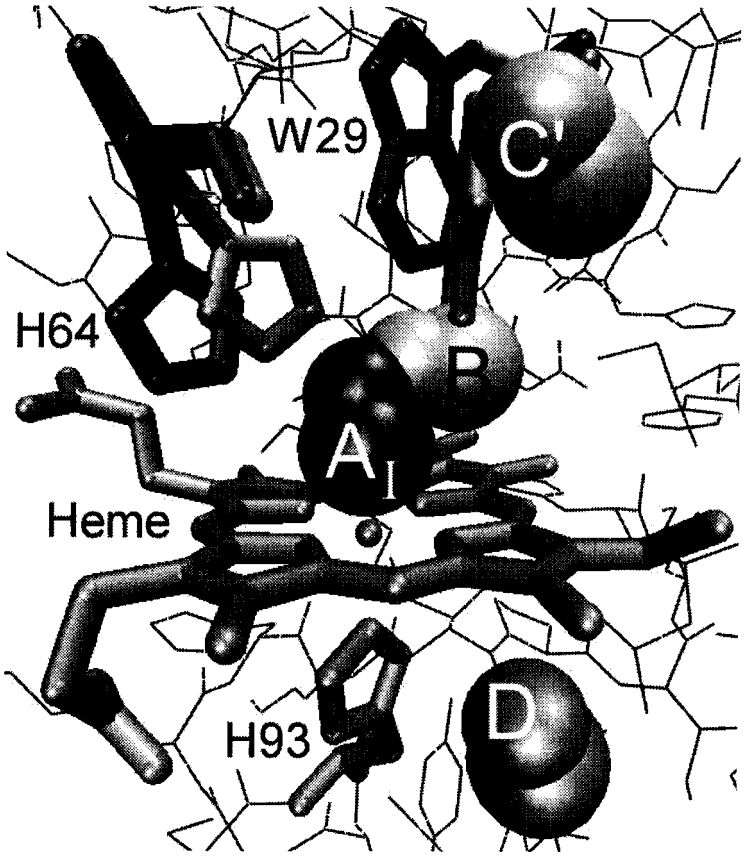

Figure 1. Model of the L29W mutant MbCO from x-ray structure analyses at 105 K [12], including the heme group and two different conformations of the sidechains of H64 and W29. They are shown in dark grey after ligand photolysis at $T < 180$ K and in light grey after ligand photolysis at $T > 180$ K. Besides the bound CO ligand (labelled A_1), the locations of the ligand in the 36 K photoproduct of native MbCO (B) [10], and in the photoproduct structure of L29W MbCO with photolysis at $T < 180$ K (C') and at $T > 180$ K (D) are shown.

sodium dithionite solution. For the spectroscopic experiments, a few microliters of the sample solution were sandwiched between two CaF_2 windows, separated by a 75 μm thick mylar washer, and mounted inside a block of oxygen-free high-conductivity copper on the cold-finger of a closed-cycle helium refrigerator (model SRDK-205AW, Sumitomo, Tokyo, Japan). The temperature was adjustable in the range between 3 and 320 K by means of a digital temperature controller (model 330, Lake Shore Cryotronics, Westerville, OH). The sample was photolyzed with a continuous wave, frequency doubled Nd-YAG laser (model Forte 530-300, Laser Quantum, Manchester, UK), operated at 300 mW output at 532 nm. Transmission

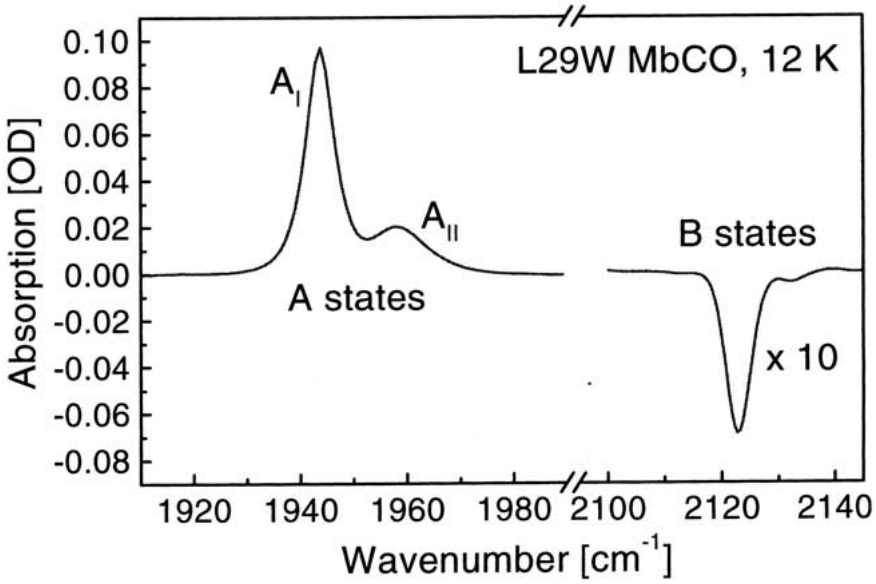

Figure 2. FTIR difference spectrum of L29W MbCO, calculated from transmittance spectra taken before and after photolysis for 1 s at 12 K. In the region of the heme-bound CO, two A substates can be distinguished, denoted by A_I and A_{II}. In the spectral region of the photodissociated CO, a dominant peak occurs at 2123 cm^{-1}.

spectra were collected in the mid-IR between 1800 cm^{-1} and 2400 cm^{-1} with a resolution of 2 cm^{-1}, using a Fourier transform infrared (FTIR) spectrometer (IFS 66v/S, Bruker, Karlsruhe, Germany).

Figure 2 shows an infrared difference spectrum of L29W MbCO in the region of the infrared stretch bands of the heme-bound and photodissociated CO at 12 K, calculated from two absorbance spectra taken before and after photolysis. Two bands are present for the heme-bound CO (near 1950 cm^{-1}); they arise from different interactions of the CO dipole with the local electric field in the distal heme pocket [17, 18], as shown experimentally by studies of many distal pocket mutants of myoglobin [19–21]. Therefore, those two bands give evidence of two so-called taxonomic substates [22] with clearly different heme pocket structures.

In L29W MbCO, we call these states A_I ($\upsilon \approx 1945$ cm^{-1}) and A_{II} ($\upsilon \approx 1958$ cm^{-1}). Below the dynamical transition temperature at ∼180 K [12, 23, 24], each molecule is frozen into one or the other substate, and thus, their relative populations are fixed, with A_I being the dominant species. Electrostatic interactions also give rise to multiple bands in the region of the photodissociated CO (above 2100 cm^{-1}), which will be discussed in detail below.

Rebinding properties of different photoproduct species were determined using temperature-derivative spectroscopy (TDS), an experimental protocol designed to investigate thermally activated rate processes with distributed barriers. The method

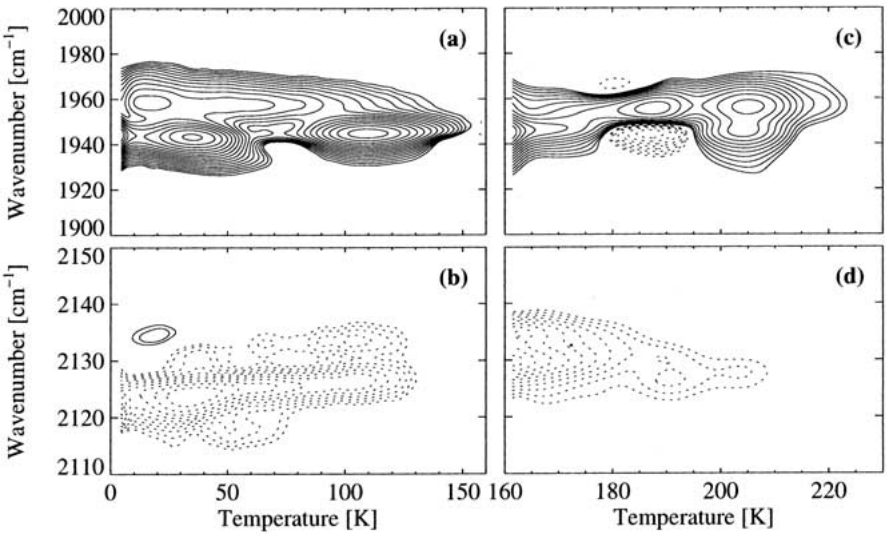

Figure 3. TDS maps of L29W MbCO following photolysis for 15,000 s at 3 K (panels a and b) and 160 K (panels c and d). Contours are spaced logarithmically, solid lines: absorbance increase, dashed lines: absorbance decrease. Top panels (a and c): absorbance changes in the A_I and A_{II} IR stretch bands of heme-bound CO; bottom panels (b and d): absorbance changes in the IR stretch bands of photodissociated CO.

has been described previously [25–27], and we give only a short summary here. The TDS measurement is started at the lowest temperature desired after preparation of the sample by laser illumination. Subsequently, FTIR transmittance spectra are taken continuously while increasing the sample temperature T at a rate of 5 mK/s. Consequently, one spectrum is collected in 200 s during which the temperature increases by 1 K. FTIR absorbance difference spectra, $\Delta A(v, T)$, are calculated from transmittance spectra, $I(v, T)$, at successive temperatures,

$$\Delta A(v, T) = \log I(v, T - \tfrac{1}{2}\mathrm{K}) - \log I(v, t + \tfrac{1}{2}\mathrm{K}). \tag{1}$$

For a particular band, the change in spectral area, $\Delta A(v, T)$, that occurs during acquisition of two successive spectra is proportional to the change in the population, ΔN, contributing to the band. Absorption changes can arise from ligand rebinding, CO diffusion among different docking sites and conformational changes of the protein. The temperature ramp protocol ensures that rebinding occurs sequentially with respect to the height of the activation enthalpy barriers controlling the dynamics. The barrier height is approximately proportional to the ramp temperature, so that the temperature axis can be converted into an enthalpy axis. TDS data are conveniently displayed as contour plots of the absorbance change on a surface spanned by the wavenumber and temperature axes.

3. Results and Discussion

Figure 3 presents TDS contour maps from two different experiments. The first experiment (Figure 3a and b) was performed such that the sample was kept at 3 K under illumination by the photolysis laser for 15,000 s. Subsequently, spectra were acquired while ramping the temperature to 160 K in the dark. In the TDS contour map in Figure 3a, the two taxonomic substates, A_I (1945 cm^{-1}) and A_{II} (1958 cm^{-1}), are plotted with solid contours representing the absorbance increase between successive temperatures because of rebinding. In the dominant species, A_I, two discrete rebinding processes are easily distinguished (maxima at 35 and 110 K), which correspond to the two photoproduct states B and C' (see Figure 1). We note that after illumination for 1 s C' is only populated to about 1%. With 15,000 s illumination at 3 K, however, about 50% of the CO ligands in the A_I substate escape to this photoproduct state from where they cannot return. This process can be observed directly in the CO bands during illumination (data not shown). For the minority conformation, A_{II}, two separately rebinding species are not observed. The channel to the C' site is apparently blocked, most likely by the W29 indole sidechain (see Figure 1). Rebinding in A_{II} is broadly distributed from the lowest temperatures up to ~140 K, suggesting that it does not occur from a single, well-defined CO location.

In the spectral region of the photodissociated CO, Figure 3b, there are mainly dashed contours, representing loss of absorbance due to rebinding. Compared with other myoglobin mutants [28, 29], there is comparatively little spectral dispersion among the various photoproduct states in L29W MbCO. Nevertheless, it is clear from the contour plots that, at 35 and 110 K, where the B and C' photoproducts dominate rebinding, the spectra of the photodissociated states contain two separate bands. We assign them to the CO located in the photoproduct site in two opposite orientations that are energetically not equivalent, as seen from the different populations. By calculating difference spectra across the rebinding features (instead of 1 K intervals), these spectra can be obtained; they are shown in Figure 4. There are also a few positive contours visible below ~30 K; they can be assigned to reorientation of a small fraction of CO molecules within the C' (xenon 4) cavity. After photodissociation at 3 K, the two possible orientations of CO in the C' cavity are not in thermal equilibrium. Initially, however, thermal energy is insufficient to overcome the barrier opposing rotation. The temperature of 20 K appears to be typical for CO movement within myoglobin, as seen in several other examples [27, 28, 30].

A second TDS experiment was performed after illuminating the sample again for 15,000 s, but this time at 160 K. Contour maps are shown in Figure 3c and d. Whereas upon photolysis at 3 K, no rebinding is observed between 160 and 230 K, substantial rebinding takes place after illumination at 160 K, suggesting that the ligand migrates to different sites with even higher barriers to recombination. Three different features can be distinguished in the A substate map in Figure 3c. From

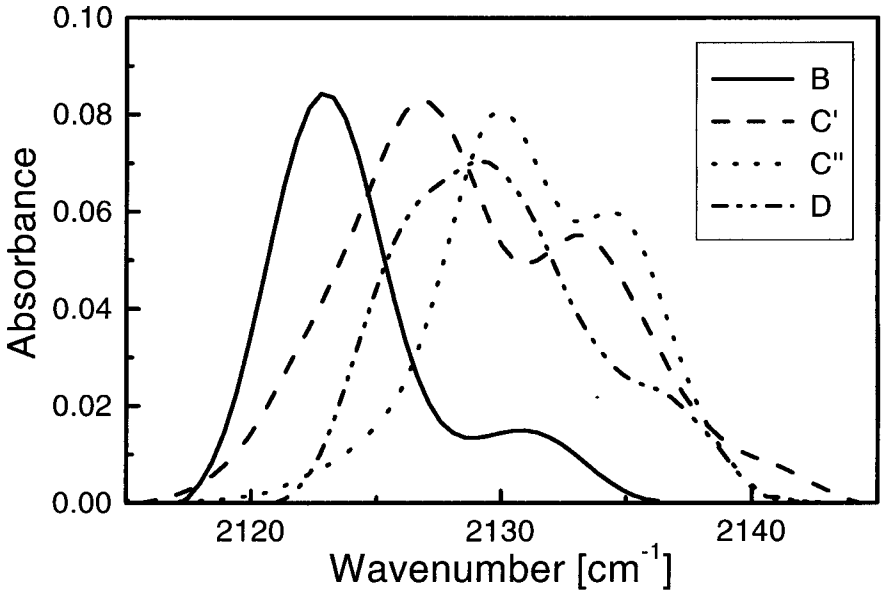

Figure 4. FTIR difference spectra associated with the different photoproduct intermediates of the A_I substate, determined from the TDS data in Figure 3 by taking differences between 30 and 40 K (B), 110 and 120 K (C'), 165 and 175 K (C'') and 190 and 200 K (D). The contribution of the A_{II} substate has been subtracted from the B spectrum. We also note that the spectra of C'' and D are identical for A_I and A_{II}.

160 to 180 K, there is recombination from an intermediate state, which we denote with C''. It clearly differs from C' because the two photoproducts rebind at different temperatures and their IR spectra of the photodissociated CO are distinctly different (Figure 4). Again, a doublet of IR bands appears, and close inspection of the contour map, Figure 3d, shows that the two peaks merge with increasing temperature. This suggests very fast CO dynamics in the C'' location, making the two orientations spectroscopically indistinguishable at $T \approx 180$ K. Another interesting observation can be made when observing the evolution of the CO spectra during the illumination period. Unlike the C' photoproduct state, C'' is significantly populated by molecules in the A_{II} bound-state structure; these, however, do not rebind between 160 and 180 K in the subsequent TDS measurement.

Between 180 and 195 K, the A substate map shows both positive and negative contours, the latter representing a decrease in absorption from a net transfer of population from the A_I to the A_{II} substate. This is a clear indication of the dynamical transition at ~180 K, above which global conformational changes can occur. The population transfer occurs because, at 180 K, a large fraction of molecules from the A_{II} substate are still photolyzed, and thus A_I and A_{II} are not populated according to equilibrium. Concomitant with the A substate exchange, a marked spectral change is observed in the map of the photodissociated CO (Figure 3d).

This is evidence that the CO, which had been accumulated in the C'' state upon illumination, migrates to a different location as protein motions set in. We note that very little rebinding occurs between 180 and 190 K. Above 190 K, Figure 3c shows a pronounced peak, which represents mainly rebinding from photoproduct state D (Figure 1) [12]. The spectrum of this intermediate (Figure 4) is rather broad, which reflects the presence of significant fluctuations within the Xe1 cavity above the dynamical transition temperature. Furthermore, we know that not all free ligands reside in D, but some escape to other sites on the protein surface or in the solvent, from where they may contribute with broad components to the CO spectra.

4. Conclusions

In this work, migration of CO through myoglobin has been investigated using FTIR spectroscopy in the CO infrared stretch bands in combination with temperature derivative spectroscopy. By extended illumination at different temperatures, we were able to accumulate populations in four photoproduct states, B, C', C'', and D associated with the A_I substate of L29W MbCO. Except for C'', the CO locations have been determined by x-ray crystallography [10, 12]. It is currently not clear how the different photoproduct sites are connected. For example, we do not know if state D is a trap state from which the ligand has to return to the distal side before exiting the protein. At physiological temperatures, there will be ligand movements among the various cavities, and in addition, fluctuations between the global A_I and A_{II} conformations, making the kinetic scheme quite complicated. These problems will be addressed in future studies using flash photolysis with infrared monitoring [31].

Acknowledgements

We thank P. Deng, Dr D.C. Lamb, O. Minkow, U. Theilen, and R. Waschipky for their collaboration. This work was supported by the Deutsche Forschungsgemeinschaft (DFG, grants GRK 328 and Ni-291/3-1).

References

1. Antonini, E. and Brunori, M.: *Hemoglobin and Myoglobin in their Reactions with Ligands*, North-Holland, Amsterdam, 1971.
2. Dickerson, R.E. and Geis, I.: *Hemoglobin: Structure, Function, Evolution, and Pathology*, Benjamin/Cummings, Menlo Park, CA, 1983.
3. Stryer, L.: *Biochemistry,* Freeman Publications, San Francisco, Fourth edition, 1995.
4. Austin, R.H., Beeson, K.W., Eisenstein, L., Frauenfelder, H. and Gunsalus, I.C.: Dynamics of Ligand Binding to Myoglobin, *Biochemistry* **14**, (1975), 5355–5373.
5. Elber, R. and Karplus, M.: Enhanced Sampling in Molecular Dynamics: Use of the Time-dependent Hartree Approximation for a Simulation of Carbon Monoxide Diffusion through Myoglobin. *J. Am. Chem. Soc.* **112** (1990), 9161–9175.

6. Scott, E.E. and Gibson, Q.H.: Ligand Migration in Sperm Whale Myoglobin, *Biochemistry* **36** (1997), 11909–11917.
7. Tilton, R.F., Kuntz, I.D. and Petsko, G.A.: Cavities in Proteins: Structure of a Metmyoglobin-xenon Complex Solved to 1.9 Å Resolution, *Biochemistry* **23** (1984), 2849–2857.
8. Schlichting, I., Berendzen, J., Phillips, G.N. and Sweet, R.M.: Crystal Structure of Photolysed Carbonmonoxy-myoglobin, *Nature* **371** (1994), 808–812.
9. Teng, T., Srajer, V. and Moffat, K.: Photolysis-Induced Structural Changes in Single Crystals of Carbonmonoxy Myoglobin at 40 K, *Nature Struct. Biol.* **1** (1994), 701–705.
10. Hartmann, H., Zinser, S., Komninos, P., Schneider, R.T., Nienhaus, G.U. and Parak, F.: X-ray Structure Determination of a Metastable State of Carbonmonoxy Myoglobin after Photodissociation, *Proc. Natl. Acad. Sci. USA* **93** (1996), 7013–7016.
11. Brunori, M., Vallone, B., Cutruzzolà, F., Travaglini-Allocatelli, C., Berendzen, J., Chu, K., Sweet, R.M. and Schlichting, I.: The Role of Cavities in Protein Dynamics: Crystal Structure of a Photolytic Intermediate of a Mutant Myoglobin, *Proc. Natl. Acad. Sci. USA* **97** (2000), 2058–2063.
12. Ostermann, A., Waschipky, R., Parak, F.G. and Nienhaus, G.U.: Ligand Binding and Conformational Motions in Myoglobin, *Nature* **404** (2000), 205–208.
13. Chu, K., Vojtchovsky, J., McMahon, B.H., Sweet, R.M., Berendzen, J. and Schlichting, I.: Structure of a Ligand-Binding Intermediate in Wild-Type Carbonmonoxy Myoglobin, *Nature* **403** (2000), 921–923.
14. Hirota, S., Li, T., Phillips, G.N., Olson, J.S., Mukai, M. and Kitagawa, T.: Perturbation of the Fe-O_2 Bond by Nearby Residues in Heme Pocket: Observation of υ_{Fe-O_2} Raman Bands for Oxymyoglobin Mutants, *J. Am. Chem. Soc.* **118** (1996), 7845–7846.
15. Šrajer, V., Teng, T., Ursby, T., Pradervand, C., Ren, Z., Adachi, S., Schildkamp, W., Bourgeois, D., Wulff, M. and Moffat, K.: Photolysis of the Carbon Monoxide Complex of Myoglobin: Nanosecond Time-Resolved Crystallography, *Science* **274** (1996), 1726–1729.
16. Springer, B.A., Egeberg, K.D., Sligar, S.G., ROWS, R.J., Mathews, A.J. and Olson, J.S.: Discrimination Between Oxygen and Carbon Monoxide and Inhibition of Autooxidation by Myoglobin. Site-Directed Mutagenesis of the Distal Histidine, *J. Biol. Chem.* **264** (1989), 3057–3060.
17. Oldfield, E., Guo, K., Augspurger, J.D. and Dykstra, C.E.: A Molecular Model for the Major Conformational Substates in Heme Proteins, *J. Am. Chem. Soc.* **113** (1991), 7537–7541.
18. Kushkuley, B. and Stavrov, S.S.: Theoretical Study of the Distal-Side Steric and Electrostatic Effects on the Vibrational Characteristics of the FeCO Unit of the Carbonylheme Proteins and Their Models, *Biophys. J.* **70** (1996), 1214–1229.
19. Braunstein, D.P., Chu, K., Egeberg, K.D., Frauenfelder, H., Mourant, J.R., Nienhaus, G.U., Ormos, P., Sligar, S.G., Springer, B.A. and Young, R.D.: Ligand Binding to Heme Proteins: III. FTIR studies of His-E7 and Val-E11 Mutants of Carbonmonoxymyoglobin, *Biophys. J.* **65** (1993), 2447–2454.
20. Li, T., Quillin, M.L., Phillips, G.N. and Olson, J.S.: Structural Determinants of the Stretching Frequency of CO Bound to Myoglobin, *Biochemistry* **33** (1994), 1433–1446.
21. Phillips, G.N., Teodoro, M.L., Li, T., Smith, B. and Olson, J.S.: Bound CO is a Molecular Probe of Electrostatic Potential in the Distal Pocket of Myoglobin, *J. Phys. Chem. B* **103** (1999), 8817–8829.
22. Frauenfelder, H., Sligar, S.G. and Wolynes, P.G.: The Energy Landscapes and Motions of Proteins, *Science* **254** (1991), 1598–1603.
23. Nienhaus, G.U., Heinzl, J., Huenges, E. and Parak, F.: Protein Crystal Dynamics Studied by Time-Resolved Analysis of X-ray Diffuse Scattering, *Nature* **338** (1989), 665–666.
24. Kneller, G.R. and Smith, J.C.: Liquid-Like Side-Chain Dynamics in myoglobin, *J. Mol. Biol.* **242** (1994), 181–185.

25. Berendzen, J. and Braunstein, D.: Temperature-Derivative Spectroscopy: A Tool for Protein Dynamics, *Proc. Natl. Acad. Sci. USA* **87** (1990), 1–5.
26. Mourant, J.R., Braunstein, D.P., Chu, K., Frauenfelder, H., Nienhaus, G.U., Ormos, P. and Young, R.D.: Ligand Binding to Heme proteins: II. Transitions in the Heme Pocket of Myoglobin, *Biophys. J.* **65** (1993), 1496–1507.
27. Nienhaus, G.U., Mourant, J.R., Chu, K. and Frauenfelder, H.: Ligand Binding to Heme Proteins. The Effect of Light on Ligand Binding in Myoglobin, *Biochemistry* **33** (1994), 13413–13430.
28. Nienhaus, K., Lamb, D.C., Deng, P. and Nienhaus, G.U.: The Effect of Ligand Dynamics on Heme Electronic Transitions in Myoglobin, *Biophys. J.* (2001), submitted.
29. Lamb, D.C., Nienhaus, K., Arcovito, A., Draghi, F., Miele, A.E., Brunori, M. and Nienhaus, G.U.: Structural Dynamics of Myoglobin: Ligand Migration among Protein Cavities Studied by FTIR-TDS Spectroscopy, *J. Mol. Biol.* (2001), submitted.
30. Alben, J.O., Beece, D., Bowne, S.F., Doster, W., Eisenstein, L., Frauenfelder, H., Good, D., McDonald, J.D., Marden, M.C., Moh, P.P., Reinisch, L., Reynolds, A.H., Shyamsunder, E. and Yue, K.T.: Infrared Spectroscopy of Photodissociated Carboxymyoglobin at Low Temperatures, *Proc. Natl. Acad. Sci. USA* **79** (1982), 3744–3748.
31. Johnson, J.B., Lamb, D.C., Frauenfelder, H., Muller, J.D., McMahon, B.H., Nienhaus, G.U. and Young, R.D.: Ligand Binding to Heme Proteins. VI. Interconversion of Taxonomic Substates in Carbonmonoxy Myoglobin, *Biophys. J.* **71** (1996), 1563–1573.